

# Ballistic Spin Injection and Detection in Fe/Semiconductor/Fe Junctions

Phivos Mavropoulos, Olaf Wunnicke, and Peter H. Dederichs

*Institut für Festkörperforschung, Forschungszentrum Jülich, D-52425 Jülich, Germany*

(Dated: February 1, 2008)

We present *ab initio* calculations of the spin-dependent electronic transport in Fe/GaAs/Fe and Fe/ZnSe/Fe (001) junctions simulating the situation of a spin-injection experiment. We follow a ballistic Landauer-Büttiker approach for the calculation of the spin-dependent dc conductance in the linear-response regime, in the limit of zero temperature. We show that the bulk band structure of the leads and of the semiconductor, and even more the electronic structure of a clean and abrupt interface, are responsible for a current polarisation and a magnetoresistance ratio of almost the ideal 100%, if the transport is ballistic. In particular we study the significance of the transmission resonances caused by the presence of two interfaces.

PACS numbers: 72.25.Hg, 72.25.Mk, 73.23.Ad

## I. INTRODUCTION

The controlled spin-dependent electronic transport through magnetic/nonmagnetic heterostructures is a central issue in the rising field of spin electronics.<sup>1,2</sup> In some cases, such as spin valves or giant magnetoresistance devices, the basic-science discoveries have lead to technological applications within less than a decade. In other cases, however, as *e.g.* spin injection into the conduction band of semiconductors (SC), much remains yet to be understood and achieved, experimentally and theoretically.

The interest in spin injection from a ferromagnetic (FM) material into a semiconductor has been largely motivated by the proposed, but not yet achieved, spin field-effect transistor of Datta and Das.<sup>3</sup> There have been many tries, with increasing success, to demonstrate that such a device is feasible.<sup>4,5,6,7,8,9,10,11,12,13,14</sup> It has been already shown<sup>4,5</sup> that electrons in the conduction band of semiconductors can travel long distances without losing memory of their spin. In parallel, many attempts to achieve spin-polarised currents have been made. The use of magnetic semiconductors as leads of the junction<sup>6,7,8</sup> would be a possibility, but they have the drawback of low Curie temperature, and thus would not be applicable at room-temperature. On the other hand, the attempts to use metallic ferromagnetic contacts were at first non-promising. Efforts to use InAs-based contacts<sup>10,11,12</sup> due to their nice properties of an abrupt interface and an ohmic transition have resulted in very low current polarisation, which might sometimes even be attributed to stray-field Hall or magnetoresistance effects.<sup>15</sup> Several theoretical approaches based on the spin-diffusion or the Boltzmann equation have shed light on the behaviour of such systems.<sup>16,17,18,19</sup> Recently Schmidt *et al.*<sup>17</sup> revealed a basic obstacle for succesful spin injection, namely the conductivity mismatch between the FM and the SC, resulting in too low current polarisation unless the FM contact is almost 100% spin polarised. Their conclusion holds in the diffusive regime, when one can use a resistor model for the FM/SC/FM heterostructure. To overcome this fundamental difficulty, Rashba<sup>18</sup> and Fert and Jaffres<sup>19</sup> have proposed that the FM and SC parts

should be separated by a tunneling spin-polarising slab, the high resistance of which would balance the drawback of the conductivity mismatch of a direct contact. In parallel, and independently from these suggestions, there has been the observation of Grundler<sup>20</sup> that a ballistic transistor would allow for a higher current polarisation than a diffusive one, and that this should be realisable if a two-dimensional electron gas was used. Already, simple model calculations,<sup>20,21,22</sup> based on a free-electron approach of the electronic structure of the leads, have shown that ballistic transport can give spin injection efficiencies of a few percent. Much more is seen, though, when one takes into account the full band structure of the FM material and the self-consistent electronic structure of the interface. Indeed, as first proposed by Kirczenow,<sup>23</sup> one can have ideal spin filters if the FM Fermi surface of only the one spin direction, when projected to the plane of the interface, has no states in the part of the two-dimensional Brillouin zone where the conduction band starts, so that there is no propagation into the SC from this spin channel. This “selection rule” unfortunately does not apply in certain interesting systems such as Fe/GaAs or Fe/ZnSe. Nevertheless, as shown by Wunnicke *et al.*,<sup>24</sup> in these systems the interface reflectance is so much different for the two spin directions that one gets spin injection ratios as high as 99% in an *ab initio* ballistic calculation. Apart from the theoretical efforts, there are some very encouraging recent experiments of Zhu *et al.*<sup>14</sup> giving already a few percent of current polarisation in Fe/GaAs(001).

In the current article we present *ab initio* calculations of ballistic spin-dependent transport in Fe/GaAs/Fe and Fe/ZnSe/Fe trilayer heterostructures grown epitaxially in the <001> direction emulating a spin-valve geometry. In this way we extend the work of Wunnicke *et al.*<sup>24</sup> to include spin injection *and* detection. We show that the presence of the two spin-filtering interfaces increases the current polarisation even closer to the ideal 100%, and we also calculate the high magnetoresistance ratios of these structures, which is also approaching the ideal 100%. We observe interesting interference effects due to the presence of two interfaces, and give an aspect of the whole problem that brings it in close connection with the

theory of magnetic tunnel junctions as it is described in Refs. 25 and 26. Our results thus stress that epitaxial junctions operating as close as possible to the ballistic regime can form almost ideal spin filters and can exhibit extremely high magnetoresistance ratios.

The article is organised as follows: in Section II we present the basic formulae of our *ab initio* approach. In Section III we describe the junctions to be calculated and the approximations made. The role of the symmetry of the wavefunctions in transport through Fe/SC/Fe junctions is explained in Section IV. Sections V and VI contain the results for the current spin polarisation and a discussion of interesting interference resonance effects, while Section VII is devoted on the case of antiparallel orientation of the leads and the magnetoresistance properties. Finally we discuss the limitations of our approach and conclude with a summary in Section VIII.

## II. METHOD OF CALCULATION

Our calculations are based on density-functional theory in the local spin density approximation (LDA). We employ the screened Korringa-Kohn-Rostoker (KKR) Green's function method<sup>27</sup> to calculate the electronic structure of the systems. In this multiple-scattering approach, the one-electron retarded Green's function at energy  $E$  is written in terms of local wavefunctions  $R_L^n(\mathbf{r})$  and  $H_L^n(\mathbf{r})$  (regular and irregular solutions of the single-site Schrödinger equation, respectively, characterised by the angular momentum index  $L = (l, m)$ ), centered at lattice sites  $\mathbf{R}_n$  and  $\mathbf{R}_{n'}$ , as

$$\begin{aligned} G(\mathbf{R}_n + \mathbf{r}, \mathbf{R}_{n'} + \mathbf{r}') \\ = -i\sqrt{E} \sum_L R_L^n(\mathbf{r}_{<}) H_L^{n'}(\mathbf{r}_{>}) \delta_{nn'} \\ + \sum_{LL'} R_L^n(\mathbf{r}) G_{LL'}^{nn'}(E) R_{L'}^{n'}(\mathbf{r}') \end{aligned} \quad (1)$$

with  $G_{LL'}^{nn'}(E)$  the so-called structural Green's function describing the intersite propagation;  $\mathbf{r}_{<}$  and  $\mathbf{r}_{>}$  are respectively the shorter and longer of  $\mathbf{r}$  and  $\mathbf{r}'$ , and atomic units have been used ( $e = -\sqrt{2}$ ,  $\hbar = 1$ ,  $m = 1/2$ ). The structural Green's function is related in turn to the known Green's function of a reference system via an algebraic Dyson equation. For more details on this we refer the reader to Refs. 28 and 29.

The systems consist of two half-infinite (Fe) leads, assumed to have perfect periodicity otherwise. Sandwiched between these leads is an “interaction” region where a different material (SC) can be placed and where the scattering of the Bloch waves takes place. The interaction region and the two leads have common in-plane Bravais vectors, *i.e.* in-plane ( $x$ - $y$ ) periodicity (perpendicular to the growth direction). If needed, larger (non-primitive)

two-dimensional unit cells are taken to match the lattice constants of the materials. The two-dimensional periodicity of the layered systems allows to Fourier-transform the Green's function in the  $x$  and  $y$  directions, obtaining a two-dimensional Bloch vector  $\mathbf{k}_{\parallel} = (k_x, k_y)$  as a good quantum number, and retaining an index  $i$  to characterise the layer in the direction of growth  $z$ . The Green's function connecting the layers  $i$  in the left lead and  $i'$  in the right lead is then written

$$\begin{aligned} G(\mathbf{R}_i + \chi_{\nu} + \mathbf{r}, \mathbf{R}_{i'} + \chi_{\nu'} + \mathbf{r}') \\ = \frac{1}{4\pi^2 S_{\text{SBZ}}} \int_{\text{SBZ}} d^2 k_{\parallel} e^{i\mathbf{k}_{\parallel}(\chi_{\nu} - \chi_{\nu'})} \\ \times \sum_{LL'} R_L^i(\mathbf{r}) G_{LL'}^{ii'}(\mathbf{k}_{\parallel}; E) R_{L'}^{i'}(\mathbf{r}') \end{aligned} \quad (2)$$

where  $\chi_{\nu}$  and  $\chi_{\nu'}$  are in-plane lattice vectors,  $\mathbf{R}_i$  is the interlayer lattice vector, SBZ is the surface Brillouin zone of the system and  $S_{\text{SBZ}}$  its area. In this equation each layer  $i$  is assumed to have a unique atom type, hence only the index  $i$  suffices to characterise the local wavefunction. In the case of more inequivalent atoms per layer, an extra index is introduced to account for the propagation between different kinds of atoms. Moreover, in the case of ferromagnetism, the Green's function is different for each spin direction  $\sigma = \uparrow$  or  $\downarrow$ .

For the calculation of the conductance in linear response all the information needed is contained in the Green's function. In the Landauer-Büttiker approach,<sup>30,31</sup> which identifies the ballistic conductance  $g$  with the transmission probability of the conducting channels, one has

$$g = \frac{e^2}{2\pi\hbar} \sum_{\sigma, \mathbf{k}_{\parallel}} \sum_{\mu, \mu'} T(\mathbf{k}_{\parallel}, \mu, \mu', \sigma) \quad (3)$$

relating the transmission probability  $T$  per channel to the conductance  $g$ . Here each channel is characterised by the band index  $\mu$ , the  $\mathbf{k}_{\parallel}$ -vector and the spin  $\sigma$  of the incoming electrons, and similarly by the primed indices for the outgoing electrons, both having the same Fermi energy  $E_F$ . Conservation of spin due to assumed absence of spin-orbit scattering, and of  $\mathbf{k}_{\parallel}$  due to two-dimensional periodicity, have allowed us to omit the summation over  $\sigma'$  and  $\mathbf{k}_{\parallel}'$  in the outgoing electron channels. We follow here the formalism of Baranger and Stone,<sup>32</sup> relating  $g$  to the spatial derivative of the Green's function connecting a cross-sectional plane in the left lead ( $L$ ) to one in the right lead ( $R$ ). It is assumed that these planes lie in the asymptotic regime, where interface perturbations and evanescent interface states are no longer present. The formula for the  $\mathbf{k}_{\parallel}$ -projected conductance  $g(\mathbf{k}_{\parallel}, \sigma)$  per two-dimensional unit cell surface area and spin  $\sigma$  reads

$$g(\mathbf{k}_{\parallel}, \sigma) = -\frac{1}{4\pi^3} \int_L d^2r \int_R d^2r' G_{\sigma}(\mathbf{r}, \mathbf{r}'; \mathbf{k}_{\parallel}; E_F) \overleftrightarrow{\partial}_z \overleftrightarrow{\partial}_z G_{\sigma}^*(\mathbf{r}, \mathbf{r}'; \mathbf{k}_{\parallel}; E_F) \quad (4)$$

where the symbol  $\overleftrightarrow{\partial}_z$  stands for

$$f(\mathbf{r}) \overleftrightarrow{\partial}_z g(\mathbf{r}) = f(\mathbf{r}) \partial_z g(\mathbf{r}) - (\partial_z f(\mathbf{r})) g(\mathbf{r}). \quad (5)$$

The conductance is evaluated only at the Fermi level  $E_F$  since we are at the limit of zero temperature. The complex conjugation in the last term of eq. (4) comes from conversion of the advanced Green's function to the retarded one by conjugation and exchange of  $\mathbf{r}$  and  $\mathbf{r}'$ .  $G(\mathbf{r}, \mathbf{r}'; \mathbf{k}_{\parallel})$  is given by the two-dimensional Fourier transform of (2). By virtue of the Fourier transformation, the integration in (4) is not performed over the whole lead cross-sectional area, but only over a two-dimensional unit cell. The total conductance per two-dimensional unit cell surface area for each spin channel is then

$$g_{\sigma} = \int_{\text{SBZ}} d^2k_{\parallel} g(\mathbf{k}_{\parallel}, \sigma). \quad (6)$$

Current conservation guarantees that the result is independent of the position of the cross-sectional planes of integration, as long as they are chosen in the asymptotic region. Details about the evaluation of the conductance will be given elsewhere.<sup>33</sup>

The formula we use for the conductance has been proven to be equivalent to the Landauer-Büttiker formula.<sup>32</sup> The conductance we calculate is then fully ballistic; diffuse scattering is assumed to be absent. Our approach also ignores spin-orbit scattering and any spin-flip events. We must also note that the semiconductor band gaps are known to be underestimated in the LDA by a factor of about 50%. This can have some quantitative significance, but the trends of our results are expected to remain unaltered even if we choose to enlarge the gap artificially.

In the calculations, the atomic sphere approximation (ASA) for the potentials is used, *i.e.* they are assumed to be spherically symmetric around each atomic site and to occupy an atomic volume; on the other hand, the full charge density, rather than its spherically symmetric part, is taken into account. Moreover, we treat the systems nonrelativistically. An angular momentum cut-off of  $l_{\text{max}} = 2$  has been taken for the wavefunctions and Green's functions in the self-consistency procedure.

### III. THE SYSTEMS UNDER STUDY

We study the spin-dependent transport through Fe/GaAs/Fe and Fe/ZnSe/Fe junctions. The junctions are supposed to have grown epitaxially on (001) interfaces, and in an ideal way so that the transition from one material to another is abrupt. Absence of interdiffusion and of disorder are assumed; in this way, we are dealing

with a system grown in the  $z$  direction and being translationally invariant in the  $x$  and  $y$  directions. The Fe leads are supposed to be infinite, while the semiconductor thickness is varied from 41 to 97 monolayers (ML). In such thicknesses, the evanescent interface states in the semiconductor are expected to have decayed to insignificance compared with the Bloch wavefunctions, so the transport will be mediated through propagating states.

Throughout the system, the experimental Fe lattice constant of  $a_{\text{Fe}} = 2.871 \text{ \AA}$  is used. Thus, all atoms sit on ideal positions of an underlying bcc lattice. In particular, in the SC part, the zincblende structure can be easily seen to fit on such a lattice, with half of the bcc sites occupied by Zn and Se (or Ga and As) atoms and the rest occupied by vacancies. Viewed in this way the consecutive positions of the atoms in the cubic diagonal of the bcc lattice are (Zn, Se, vacancy, vacancy). The zincblende lattice constant is then twice the one of the bcc. One can see, that using  $2 \times a_{\text{Fe}} = 5.742 \text{ \AA}$  in the SC part results only in a slight mismatch of less than 2%, the experimental lattice constants being  $5.654 \text{ \AA}$  for GaAs and  $5.670 \text{ \AA}$  for ZnSe. In all cases, Zn termination of the ZnSe spacer and Ga termination of the GaAs spacer was considered. As shown in Ref. 24, the spin polarisation of the current through the single interface for the other terminations (Se and As) is also extremely high, and from the analysis of Sections V-VII it follows that the two-interface junctions for those terminations will have qualitatively the same properties as the ones studied here. The two planes  $L$  and  $R$  used for the integration were 6MLs away from the interfaces in the Fe region, where the asymptotic regime is assumed to have been reached. Variation of this distance causes insignificant changes in the results.

In a system as the ones we are considering, the Fermi level will be naturally determined by the infinitely long Fe leads. But in the spacer material, two or three monolayers after the interface, the potentials and the charge density must be almost bulk-like. For this reason, the potentials of the inner atoms of the spacer will be automatically adjusted to the Fe Fermi level by a constant shift which is the result of the interface dipole layer. The self-consistent calculation of the potential close to the interface is then essential.

Since we want to inject electrons into the SC conduction band, we must emulate in some way a gate voltage, or energy shift, acting on the SC potentials in order to lower the conduction band minimum slightly under the Fermi level. This artificial shift is different than the one just mentioned above, and it enters as a parameter in our calculations. We avoid disturbing the interface electronic structure, which is strongly influenced by the

metal-induced gap states, and proceed as follows.<sup>24</sup> The first two SC monolayers adjacent to the interface are kept as calculated by a self-consistent calculation of a 9ML-thick SC slab sandwiched between infinite Fe leads. The same applies also for the first neighbouring Fe MLs. Having saved the interface in this way, we take for the rest of the SC spacer (third up to last-but-two ML) the bulk-like potential that we find for the atoms in the middle of this Fe/9ML SC/Fe junction. This is justified, since it is known that the potential stabilises quickly as mentioned previously. The emulation of the gate voltage is achieved by applying to this potential an extra shift such that the conduction band minimum  $E_c$  of this bulk-like structure falls slightly under the Fermi level  $E_F$  of the whole structure:

$$E_F = E_c + E_0. \quad (7)$$

The parameter  $E_0$ , characterising the assumed gate voltage, is varied in our calculations over three values: 20mRy, 10mRy, and 5mRy (272meV, 136meV and 68meV, respectively). In this way we are able to view the approach to small values as a limiting procedure; as we shall see, these values are already in the limit of large spin polarisation of the current and magnetoresistance. Viewing the semiconductor part, the small values of  $E_0$  mean that the energy dispersion relation is nearly parabolic,

$$E(\mathbf{k}) - E_c \simeq \frac{1}{m^*} \mathbf{k}^2 = \frac{1}{m^*} (\mathbf{k}_{\parallel}^2 + k_z^2) \quad (8)$$

where  $m^* = (\partial^2 E / \partial k^2)^{-1}$  is the effective mass, and that the Fermi wavenumber  $k_F$  is very small:

$$E_F - E_c = E_0 = \frac{1}{m^*} k_F^2 = \frac{1}{m^*} (\mathbf{k}_{\parallel}^2 + k_z^2). \quad (9)$$

These relations are relevant in the semiconductors considered here because of their direct band gap at the  $\Gamma$ -point. Because  $E_0$  is very small, we have a very small Fermi sphere in the semiconductor. For this reason, very few channels  $\mathbf{k}_{\parallel}$  will be able to conduct, namely those close to the center of the Brillouin zone with  $|\mathbf{k}_{\parallel}| \leq k_F$ . For the rest  $k_z$  becomes imaginary and represents decaying wavefunctions. These can give rise to a tunneling current, but for the larger spacer thicknesses they are small compared to the contribution from the central part of the Brillouin zone. In any case they are always included in the calculation.

#### IV. THE IMPORTANCE OF SYMMETRY

As mentioned in the previous section, we are expecting contributions to the current only from the central part of the (001) Surface Brillouin Zone (SBZ), *i.e.* from  $\mathbf{k}_{\parallel}$  close to the  $\bar{\Gamma}$ -point. In view of this, we will examine the expected behaviour for states exactly at  $\mathbf{k}_{\parallel} = 0$ , and argue, and show in fact in the calculations, that by continuity the close-by states will behave similarly.

To begin with, we must clarify that the two-dimensional unit cell and the SBZ are determined by the SC part, since one SC lattice constant is assumed to match exactly two Fe lattice constants in our case. The states with  $\mathbf{k}_{\parallel} = 0$  can be examined in a great extent through their symmetry properties, since the  $z$ -axis remains invariant under many point-group operations. The single Fe (001) surface is characterised by the symmetry group  $C_{4v}$ , having eight operations: a fourfold rotation axis (here the  $z$ -axis) plus reflections over the planes containing the  $z$ -axis and the  $xy$  diagonal or antidiagonal. But the zincblende (001) surface has the symmetry group  $C_{2v}$ , having four operations (a twofold rotation axis plus the reflections over the  $xy$  diagonal and antidiagonal), and being a subgroup of the former. As a result, the combined Fe/SC interface is characterised by the group  $C_{2v}$ .

The idea now, in view the Landauer approach and Eq. (3), is to investigate the incoming states at the Fermi level deep in the Fe lead, as incoming channels, in order to see if their symmetry properties allow them to couple to SC propagating bulk states, and then see if these in turn are allowed (by symmetry) to couple to the outgoing states which propagate deep in the other Fe lead. The different character of the Fe states for majority and minority spin will give us in this way hints about the spin polarisation of the current. This procedure can be used to propose theoretically ideal spin filter systems. But note that in this way we can only find which channels are excluded from transmission by symmetry. As we shall see, some channels can be almost blocked for other reasons, contributing (by their absence from transmission) to the spin injection effect.

We can now turn our attention to Fig. 1, where the energy bands of Fe, ZnSe and GaAs are drawn for  $k_x = k_y = 0$  in the  $k_z$ -direction, which is the one of interest as discussed earlier. Each of them is named by the irreducible representation to which it belongs<sup>34</sup> for rotations around the  $\Delta$ -axis (*i.e.*  $k_z$ ). For example, the state labeled “1” corresponds to the  $\Delta_1$ , which means that the states are invariant under all group operations (rotations around the  $z$ -axis); the label 2' refers to the  $\Delta_{2'}$  representation, being invariant under reflections from the planes containing the  $z$ -axis and either the  $xy$  diagonal or antidiagonal. But we must note that for Fe the nomenclature refers to the  $C_{4v}$  group, while the symmetry group of the whole system as well as of the bulk semiconductor is  $C_{2v}$ . Therefore we must use the compatibility relations between the two groups, that show us which representations of  $C_{4v}$  have nonzero projection in each representation of  $C_{2v}$ . These can be found, for instance, in Ref. 34. In our case we see that, at the Fermi level, only one band exists in the semiconductor (both for GaAs and ZnSe), and it belongs to the representation  $\Delta_1(C_{2v})$  (in parentheses we specify the point group to which the representation belongs). With this representation, only the  $\Delta_1(C_{4v})$  and  $\Delta_{2'}(C_{4v})$  states of bulk Fe are compatible. This means that incident states of only

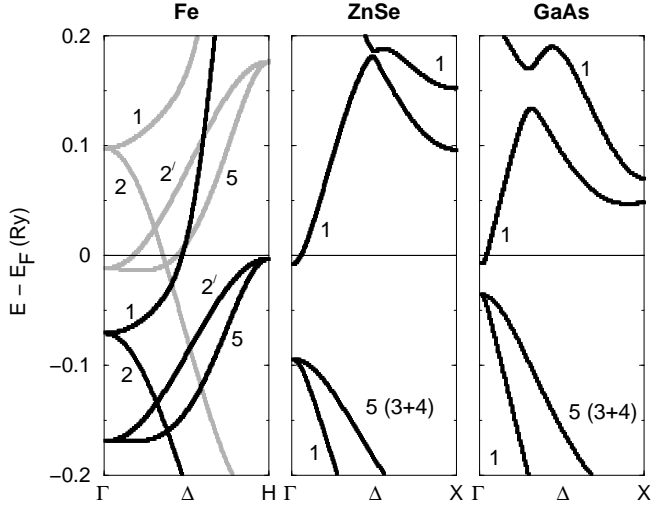


FIG. 1: Energy bands of bulk Fe (left) together with bulk ZnSe (centre) and bulk GaAs (right) along the  $\Delta$ -direction ( $k_z$ ), corresponding to  $\Gamma - H$  in bcc (Fe) and to  $\Gamma - X$  in fcc (zincblende). For Fe, the black lines represent majority-spin states, and the gray lines minority-spin states. The potentials of GaAs and ZnSe have been appropriately shifted so that the Fermi level falls slightly in the conduction band. Each band is named by the corresponding irreducible representation of the point group; *e.g.* 1 means the  $\Delta_1$  representation,  $2'$  the  $\Delta_{2'}$  etc. For the notation see, *e.g.*, Ref. 34. Note that the  $k_z$ -axes at the semiconductor plots should actually be half the size shown, since the lattice constant is assumed double the one of Fe. Backfolded bands due to the doubling of the Fe two-dimensional unit cell are unimportant and not shown.

these symmetries can couple to the semiconductor conduction states (or even to each other, near the interface) and propagate into the SC spacer, while the rest,  $\Delta_2(C_{4v})$  and  $\Delta_5(C_{4v})$ , are totally reflected at the interface.

Now, the energy bands of Fe can be quite different for majority vs. minority electrons near the Fermi level, due to the exchange splitting. At  $E_F$  the majority electrons have a  $\Delta_1(C_{4v})$ -state that can couple to the semiconductor, while this is absent for the minority-spin carriers. For these, on the other hand, a  $\Delta_{2'}(C_{4v})$ -band exists that can do the job. We note in passing that this absence of  $\Delta_1(C_{4v})$  is due to the so-called *s-d*-hybridisation gap which splits this band in two and which happens to fall around  $E_F$  for the minority-spin states.

If the  $\Delta_{2'}(C_{4v})$ -band were absent, or if it could not couple to the  $\Delta_1(C_{4v})$ -band of the semiconductor, we would be facing an ideal spin filter: only majority-spin would be able to propagate. Even in our case, however, we shall see that almost ideal spin filtering will occur, because the two kinds of states,  $\Delta_1(C_{4v})$  and  $\Delta_{2'}(C_{4v})$ , have very different transmission probabilities through the interfaces such that the  $\Delta_{2'}(C_{4v})$  channels are nearly blocked.

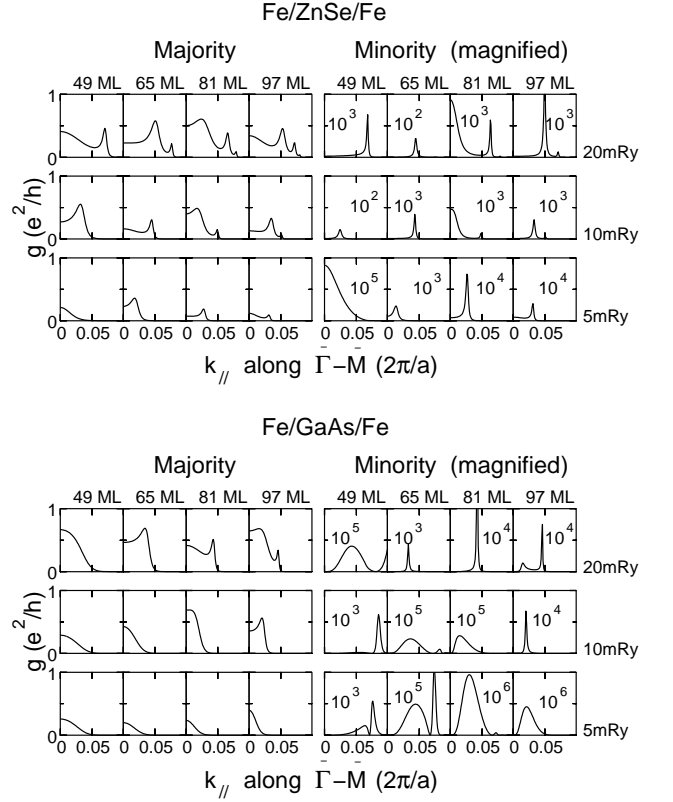


FIG. 2: Spin-dependent conductance for Fe/ZnSe/Fe (top) and Fe/GaAs/Fe (bottom) junctions, as a function of  $k_x$ , for the parallel magnetic configuration of the leads. The majority-spin conductance is illustrated in the left pannels and the minority in the right. Several SC spacer thicknesses are considered (49ML to 97ML), and gate energy shifts of  $E_0 = 5, 10$ , and  $20$  mRy. For the minority-spin case a magnification from  $10^2$  to  $10^6$  (see inset numbers) has been used to bring the graphs to the same scale. The  $k_F$ -values for ZnSe are 0.038, 0.056, and 0.083, and for GaAs 0.021, 0.031, and 0.050 for  $E_0 = 5, 10$ , and  $20$  mRy, respectively.

## V. RESULTS FOR THE SPIN-DEPENDENT CONDUCTANCE

The spin-dependent conductance as a function of  $\mathbf{k}_{\parallel}$  for several spacer thicknesses is shown in Fig. 2 for GaAs and ZnSe spacers, and for several energy shifts  $E_0$ . The wavevector  $\mathbf{k}_{\parallel}$  has been taken along the  $\Gamma$ -X cubic direction, which in the two-dimensional geometry corresponds to  $\bar{\Gamma}$ - $\bar{M}$ . It is most convenient to express  $\mathbf{k}_{\parallel}$  in units of  $2\pi/a_{SC} = 2\pi/(2a_{Fe})$ , since this corresponds to the two-dimensional periodicity of the whole system; henceforth these units will be implied but omitted for simplicity. The calculated values of  $k_F$  are given in the caption of Fig. 2.

The first evident observation is that the conductance practically vanishes for  $k_{\parallel} > k_F$ , as expected. This effect shows up clearer for the thicker spacers. Thus we can

see that, as  $E_0$  rises and the Fermi sphere in the SC becomes larger, the cutoff in conductance moves to higher values of  $k_{\parallel}$ , exactly as  $k_F$ . As mentioned earlier, for larger values only evanescent states can exist, giving rise to a very small tunneling current which dies out as the spacer gets thicker. Nevertheless our calculations show that these states dominate the behaviour in the small thickness region.

One can clearly see that the minority-spin conductance is lower by orders of magnitude than the majority counterpart. This is clearly the effect of the Fe minority  $\Delta_{2'}$ -state not being able to couple well with the SC  $\Delta_1$ -state at the interface. The reason for this is that the  $\Delta_{2'}$ -state consists locally of  $d_{xy}$ -like site-centered orbitals. These point in-plane and are quite localised, so they cannot overlap very well with the SC  $\Delta_1(C_{2v})$  orbitals. Moreover, the SC  $\Delta_1(C_{2v})$  band consists of  $s$ ,  $p_z$ , and  $d_{xy}$ -like states. The latter are in fact the ones that do couple to the  $\Delta_{2'}$  minority band of Fe. But we must note that such  $d_{xy}$ -like SC states are not inherent to the SC atoms, but rather induced as a distortion to the inherent  $sp$  SC orbitals by the neighbouring atoms sitting in the tetrahedral positions and giving a directional preference; in this sense they appear just as a correction when we use an angular momentum basis. As we depart from the  $\bar{\Gamma}$ -point, other Fe minority orbitals (the continuations of the  $\Delta_5$  and  $\Delta_2$  bands) begin to couple slowly, so the transmission increases.

In contrast, the  $\Delta_1(C_{4v})$ -band present in the majority-spin states consists locally of  $d_{z^2}$ , as well as  $s$  and  $p_z$ -like atomic orbitals; these, pointing partly into the SC and being more extended, favour a better overlap and bonding with the SC states. Thus the reflectance of the interface is by far stronger for the minority-spin electrons, and a strongly polarised current results.

The arguments presented here show that one needs a clean and abrupt interface, so that  $\mathbf{k}_{\parallel}$  is conserved. In the case of  $\mathbf{k}_{\parallel}$ -violation due to diffuse scattering the effect of spin selection will be reduced. Indeed, the total (*i.e.*  $\mathbf{k}_{\parallel}$ -integrated) density of states of Fe at  $E_F$  is higher for the minority-spin than for the majority-spin. On these grounds one would expect even a negative current polarisation, in similarity with Julliere's model<sup>35</sup> for spin-dependent tunneling; this might be the case if strong diffusive scattering intermixes the scattering  $\mathbf{k}_{\parallel}$ -channels in a completely random way. Thus it is the specific selection rule imposed by the interface in the ballistic regime that causes the strong positive current polarisation. We may also note that for other interfaces, such as (110) or (111), the symmetry of the various incident states is different than in (001), and the selection rule might not be as strong; an *ab initio* calculation is necessary in order to judge this.

Note that the same effect appears when one looks at tunneling, rather than spin injection, in these structures. This is demonstrated in Ref. 25, where the tunneling through the semiconductor is also confined to the states close to  $\bar{\Gamma}$ ; there, the majority Fe state of symmetry  $\Delta_1$

couples much better at the interface than the minority state of symmetry  $\Delta_{2'}$ , while both propagate with equal difficulty afterwards in the SC, as evident by the equal decay rate. In that case, of course, one must consider the complex band structure of ZnSe in the gap region as the analytical continuation of the conduction band of the same symmetry for the interpretation of the effect,<sup>26</sup> rather than the real conduction band structure, but both tunneling and spin injection can be viewed in this respect in a unified way.

## VI. INTERFACE REFLECTANCE AND QUANTUM WELL STATES

Another interesting feature is the multi-peaked structure of  $g(k_{\parallel})$ . This is an interference effect to the discussion of which we turn now. We start with the observation that the presence of two Fe/SC interfaces can give rise to interference effects due to the coherent multiple reflection of the electrons between them. So, one expects resonances in the transmission, similarly to the case of a square barrier of finite length met by free electrons of energy higher than the barrier.<sup>36</sup> More concretely, let us assume that the transmission through each Fe/SC interface (1 or 2) has an amplitude  $t_{1,2}$  and the reflection  $r_{1,2}$ . These contain the phase shifts  $\phi_{1,2}$ , that the wavefunction obtains for each reflection, plus a phase factor of  $e^{ik_z D}$  for the wave propagation from side to side of the SC slab of thickness  $D$  leading to a phase of  $2k_z D$  for a come-and-go. A resonance in transmission will be formed whenever there is constructive interference after a number of comes-and-goes of the wave; *i.e.* one has to sum up the series

$$\begin{aligned} t_{\text{tot}} &= t_1 t_2 + t_1 r_2 r_1 t_2 + t_1 r_2 r_1 r_2 r_1 t_2 + \dots \\ &= t_1 \frac{1}{1 - |r_1||r_2|e^{i(2k_z D + \phi_1 + \phi_2)}} t_2 \end{aligned} \quad (10)$$

in order to find the maxima in transmission. If the two interfaces are the same, as in Fe/SC/Fe with parallel magnetic orientation of the leads, the single-interface probabilities  $T_{\text{si}}$  of transmission and  $R_{\text{si}} = 1 - T_{\text{si}}$  of reflection are equal for the two interfaces (the Fe/SC interface is equally hard to cross in either direction), and by squaring the previous equation one finds the total transmission probability to be

$$\begin{aligned} T_{\text{tot}} &= |t_{\text{tot}}|^2 \\ &= \frac{T_{\text{si}}^2}{1 + (1 - T_{\text{si}})^2 - 2(1 - T_{\text{si}}) \cos(2k_z D + \phi_1 + \phi_2)} \end{aligned} \quad (11)$$

where we have used the fact that  $T_{\text{si}} = |t_1 t_2|$  is valid in this case; Eq. (12) is equivalent to the formula of Airy for a Fabry-Perot interferometer. This function is clearly oscillatory in  $k_z D$ , and it exhibits a maximum of  $T_{\text{tot}} = 1$ , *i.e.* a resonance, whenever the condition for constructive interference is met:

$$\phi_1 + \phi_2 + 2k_z D = 2\pi n, \quad (12)$$

with  $n$  an integer.

For a given thickness  $D$ , variation of  $k_{\parallel}$  will cause variation of  $k_z$ , and this will lead to these resonance phenomena.<sup>43</sup> This is realised by combining eqs. (9) and (12), so that the multi-peaked structure in Fig. 2 is explained. To see what one expects qualitatively, we combine eqs. (9) and (12) to get

$$2\sqrt{k_F^2 - k_{\parallel}^2} D = 2\pi n + \phi_1 + \phi_2 \quad (13)$$

as a resonance condition. For zinc-blende structures, where  $k$  varies between 0 and 1 in units of  $2\pi/a_{\text{SC}}$ , and  $a_{\text{SC}} = 4\text{ML}$  in the (001) direction, the condition relates  $k_{\parallel}$  to the number of monolayers  $N_{\text{ML}}$ :

$$\sqrt{k_F^2 - k_{\parallel}^2} N_{\text{ML}} = 2n + (\phi_1 + \phi_2)/\pi. \quad (14)$$

Naturally,  $\phi_1$  and  $\phi_2$  depend on  $\mathbf{k}_{\parallel}$ . This formula can be seen to give three resonances already for  $N_{\text{ML}} = 100$  and  $k_F = 0.05(2\pi/a_{\text{SC}})$ .

Between the maxima there are minima of  $T_{\text{tot}} = T_{\text{si}}^2/(2 - T_{\text{si}})^2$ . For low values of  $T_{\text{si}}$  the halfwidth of the resonance becomes very small; this is reflected at the minority-spin conductance where the resonances are much more narrow and peaked, with extremely low valued valleys between them, and thus their  $\mathbf{k}_{\parallel}$ -integrated contribution remains insignificant compared to the majority one. These arguments also demonstrate that the interference effects are in practice unable to invert the injected current polarisation, in contrast to what has been predicted by recent model calculations.<sup>44</sup> We also note that, for  $E_F \rightarrow E_C$ ,  $T_{\text{si}} \propto k_z \propto \sqrt{E_F - E_C}$ .<sup>45</sup> Then for a given spacer thickness  $T_{\text{tot}}$  goes to zero linearly as  $T_{\text{tot}} \propto E_F - E_C$ , while the first resonance appears for a thickness  $D_{\text{res}}$  increasing to infinity as  $1/\sqrt{E_F - E_C}$ . In the model described here, one can readily substitute the values of  $T_{\text{si}}$  from a single-interface calculation,<sup>24</sup> and get the correct trend.<sup>46</sup> Nevertheless, in the calculations we cannot observe a perfect resonance of transmission one, because perfect coherence is destroyed by a very small but nonzero imaginary part of the energy, numerically necessary for the calculation of the retarded Green's function.<sup>47</sup>

Another aspect of the matter is this: at the resonance values of  $k_z D$  we have also a formation of quantum well-like states in the spacer. They are not bound, since the reflection is not total; the “interactive” change in the integrated density of states for each  $\mathbf{k}_{\parallel}$  because of them, compared to the bulk Fe, is<sup>39</sup>

$$\Delta N(E) = -\frac{1}{\pi} \text{Im} \ln(1 - |r_1||r_2|e^{i(2k_z D + \phi_1 + \phi_2)}) \quad (15)$$

per spin direction. Whenever such a quantum well state is met, a resonance in the transmission probability is expected; the larger  $|r_1||r_2|$  is, the more peaked and localised in energy is the change of the DOS and the transmission resonance.<sup>48</sup>

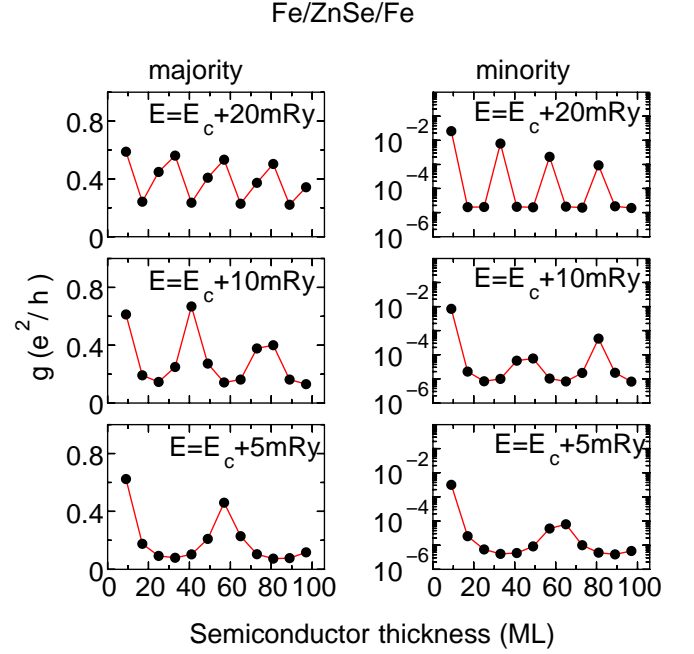


FIG. 3: Majority- (left) and minority- (right) spin conductance at  $\mathbf{k}_{\parallel} = 0$  as a function of the ZnSe spacer thickness. The oscillations of period  $2\pi/(2k_F)$  are evident; the values of  $2\pi/(2k_F)$  are 24.1ML, 35.7ML and 52.6ML for  $E_0 = 20, 10$  and 5mRy, respectively. The peaks are much more violent for the minority-spin case (note the logarithmic scale there) because of the greater confinement due to stronger interface reflection.

Dual to the oscillations of  $g$  in  $k$ -space are oscillations in real space, when the spacer thickness  $D$  is varied while  $\mathbf{k}_{\parallel}$  is kept constant. As can be read out from eq. (12), one expects a thickness period of  $2\pi/(2k_z)$ , which for  $\mathbf{k}_{\parallel} = 0$  becomes  $2\pi/(2k_F)$ . Indeed, in Figs. 3 and 4 we can see this oscillatory effect on the majority-spin conductance (left panels) for both ZnSe and GaAs spacers, with exactly the predicted period. The period gets longer for lower energy shifts, since they correspond to lower  $k_F$ . On the other hand, larger  $k_{\parallel}$  will result in larger periods, until the limit value of  $k_{\parallel} = k_F$ ; after that  $k_z$  becomes imaginary, and one has attenuation rather than propagation of the wave, described by the complex band structure, as in a tunnel junction.

Similarly, the minority-spin conductance oscillates with the same period as seen in Figs. 3 and 4 (right panels), but for the reasons mentioned before the peaks are much more pronounced; note that in this case a logarithmic scale was used for the intensities. It should be noted that there is, in particular for GaAs, an initial exponential decrease in the conductance, before the oscillations start, as can be seen from the characteristic linear behaviour in the logarithmic scale. This originates from decaying states with complex Bloch vectors, which contribute to the conductance by tunneling. In-

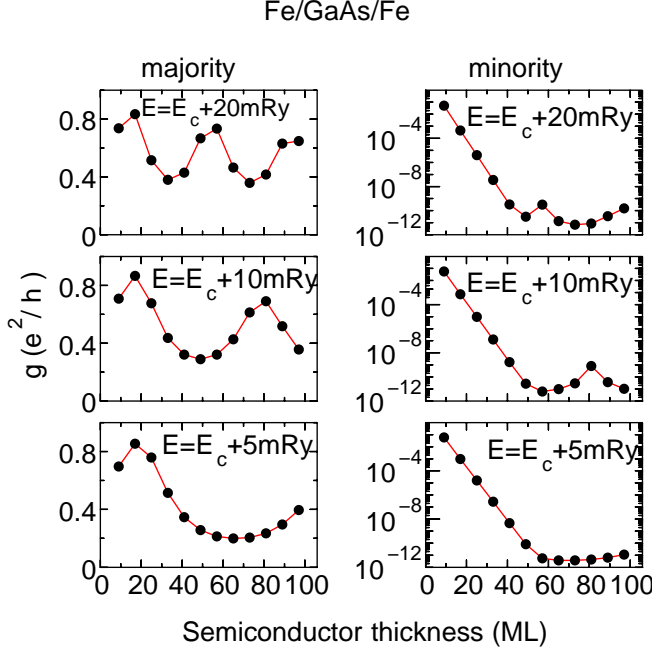


FIG. 4: Same as in Fig. 3, but for GaAs spacers. Here, the values of  $2\pi/(2k_F)$  are 40ML, 64.5ML and 95.2ML for  $E_0 = 20, 10$  and  $5\text{mRy}$ , respectively.

deed, minority-spin states incident from Fe at  $E_F$  having the  $\Delta_5(C_{4v})$  and  $\Delta_2(C_{4v})$  symmetry (see Fig. 1) cannot couple to the SC  $\Delta_1(C_{2v})$  conduction band, but they can couple to decaying SC states that have the correct symmetry. In this way, if the thickness of the spacer is moderate, they can have an important contribution to the current through tunneling.<sup>26</sup> For larger thicknesses they become unimportant, and the asymptotic oscillatory behaviour appears. This situation of co-existence of tunneling current with “normal” current is much stronger in GaAs, because it has a smaller band gap than ZnSe, and thus the decay length of such evanescent states is much longer.

In Figs. 5 and 6, the majority-spin  $g(\mathbf{k}_{\parallel})$  is demonstrated for 97ML-thick spacers of GaAs and ZnSe, for gate voltage shifts of  $E_0 = 5\text{mRy}$ ,  $10\text{mRy}$  and  $20\text{mRy}$ . The conductance resonances form rings around  $\mathbf{k}_{\parallel} = 0$ , up to  $k_F$ ; they are what one expects by rotating the graphs of Fig. 2 around the origin. It is remarkable that the majority-spin conductance is quite isotropic in all cases. In contrast, we find the minority-spin conductance rings to reflect more the quadruplicate structure of the surface Brillouin zone, but seem actually (by inspection) to obey one extra symmetry operation and to be octuple, as if the group were  $C_{4v}$ . This is observed in all cases, and is mostly evident in the case of ZnSe with  $E_0 = 20\text{mRy}$ , where  $k_F$  is largest; this is shown in Fig. 7. We shall give the explanation of these observations together with the analysis of similar data for the antiparallel magnetic configuration of the leads, at the end of the

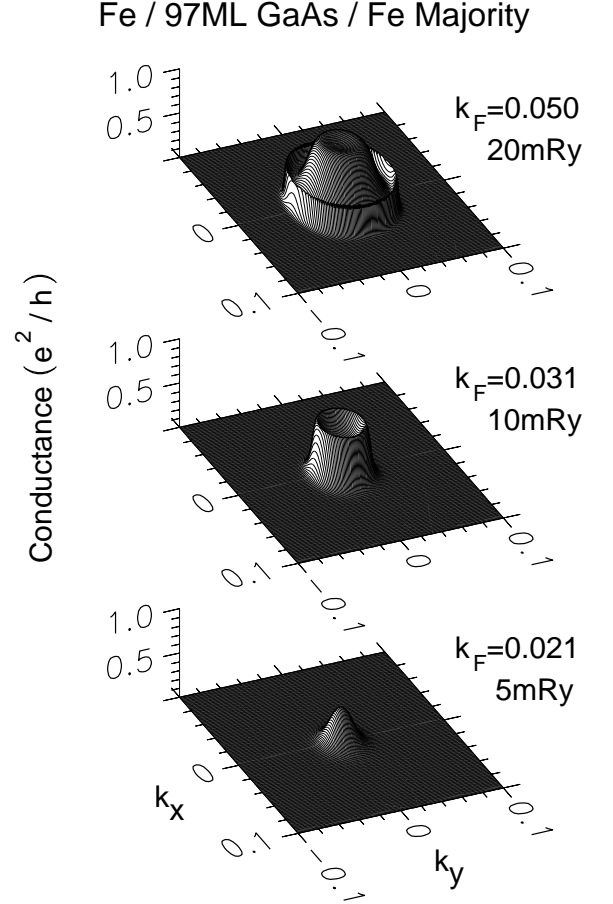


FIG. 5: Conductance ( $\mathbf{k}_{\parallel}$ -resolved) of majority-spin electrons, in the case of a Fe/ 97ML GaAs /Fe junction. Top:  $E = E_c + 20\text{mRy}$ ,  $k_F = 0.050$ ; Middle:  $E = E_c + 10\text{mRy}$ ,  $k_F = 0.031$ ; Bottom:  $E = E_c + 5\text{mRy}$ ,  $k_F = 0.021$ . The  $\mathbf{k}_{\parallel}$  axes are along the  $\bar{\Gamma} - \bar{M}$  directions.

next section. Evidently, the majority-spin conductance retains its dominance over its minority counterpart; the  $\mathbf{k}_{\parallel}$ -integrated conductance is presented in Table I.

## VII. ANTIPARALLEL MOMENT IN THE LEADS - MAGNETORESISTANCE

From the analysis presented in Sections IV and V one should expect a strong reduction of the conductance if the magnetic moments of the leads have an antiparallel orientation. If the moment of, say, the second lead is reversed, then the majority and minority bands will be interchanged there. So, the incoming minority-spin electrons will be nearly blocked at the first interface, while the incoming majority-spin electrons will propagate up to the second interface but suffer almost total reflection there, since they will encounter the states of the  $\Delta_{2'}(C_{4v})$ -type to which they do not couple well. Again



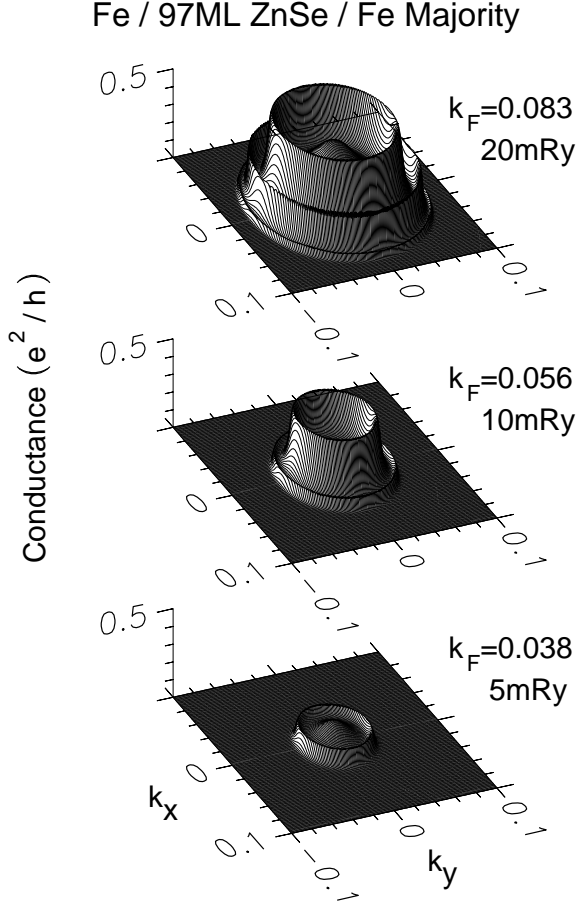


FIG. 6: Conductance ( $\mathbf{k}_{\parallel}$ -resolved) of majority-spin electrons, in the case of a Fe/ 97ML ZnSe /Fe junction. Top:  $E = E_c + 20\text{mRy}$ ,  $k_F = 0.083$ ; Middle:  $E = E_c + 10\text{mRy}$ ,  $k_F = 0.056$ ; Bottom:  $E = E_c + 5\text{mRy}$ ,  $k_F = 0.038$ . The  $\mathbf{k}_{\parallel}$  axes are along the  $\bar{\Gamma} - \bar{M}$  directions.

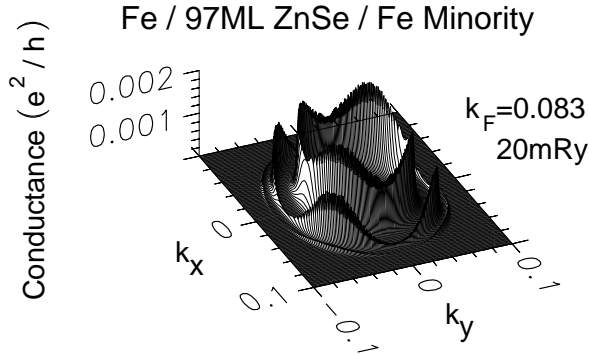


FIG. 7: Conductance ( $\mathbf{k}_{\parallel}$ -resolved) of minority-spin electrons, in the case of a Fe/ 97ML ZnSe /Fe junction for  $E = E_c + 20\text{mRy}$ ,  $k_F = 0.083$ ; an octuple symmetry is evident. The  $\mathbf{k}_{\parallel}$  axes are along the  $\bar{\Gamma} - \bar{M}$  directions.

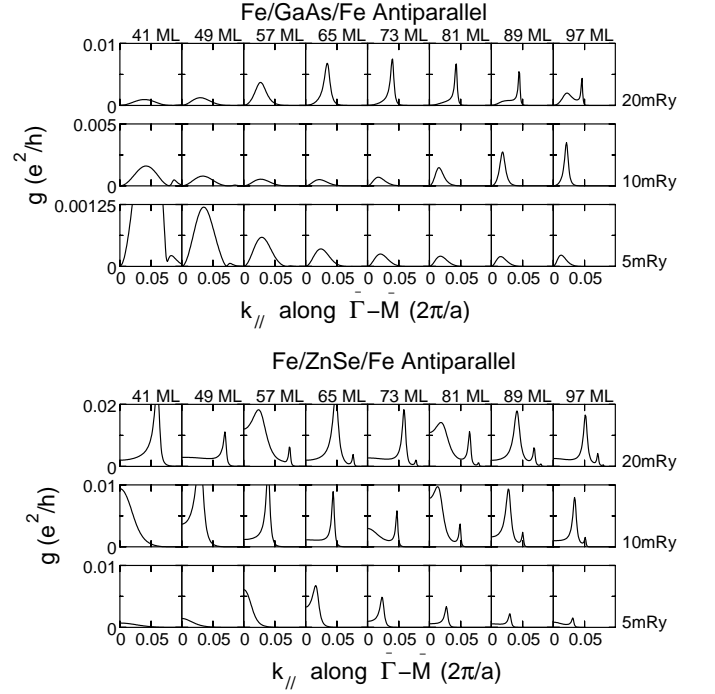


FIG. 8: Fe/GaAs/Fe (top) and Fe/ZnSe/Fe (bottom) conductance per spin channel along  $\bar{\Gamma} - \bar{M}$  ( $k_x$ ), for the antiparallel magnetic configuration of the leads, and for several spacer thicknesses. The values are much lower than the majority-spin conductance and much higher than the minority-spin conductance in the parallel case. The  $k_F$ -values are: 0.021, 0.031, and 0.050 for  $E_0 = 5, 10$ , and  $20\text{mRy}$ , respectively.

the situation is analogous to the one encountered in the case of tunneling barriers.<sup>25</sup>

Indeed, in Fig. 8 we see that the conductance in the antiparallel configuration is calculated to be orders of magnitude lower than the majority-spin conductance (and the total one) of the parallel configuration, but still orders of magnitude higher than the minority-spin conductance of the parallel configuration. The effect can be understood in terms of the reflectance and transmittance at the interfaces. If  $T_{\text{si}}^{\uparrow}$  is the (high) single-interface transmission probability involving majority Fe states and  $T_{\text{si}}^{\downarrow}$  is the (low) one involving minority Fe states, with  $T_{\text{si}}^{\uparrow} \gg T_{\text{si}}^{\downarrow}$ , then in the case of parallel alignment the majority electrons will have a total transmission probability from both interfaces of the order of  $T_{\text{tot}} \sim (T_{\text{si}}^{\uparrow})^2$  (neglecting resonance effects), the minority ones  $(T_{\text{si}}^{\downarrow})^2$ , while the antiparallel-configuration electrons will have  $T_{\text{si}}^{\uparrow} T_{\text{si}}^{\downarrow}$  for each spin channel. Evidently,  $(T_{\text{si}}^{\uparrow})^2 \gg T_{\text{si}}^{\uparrow} T_{\text{si}}^{\downarrow} \gg (T_{\text{si}}^{\downarrow})^2$ , *q.e.d.* We observe, by the way, that this line of thought suggests that in the antiparallel configuration the conductance  $g_{\uparrow\downarrow}$  (per spin channel) is the geometrical average of the conductances of the two spin channels in the parallel case:  $g_{\uparrow\downarrow} = \sqrt{g_{\uparrow\uparrow} g_{\downarrow\downarrow}}$  (to be valid but for backscat-

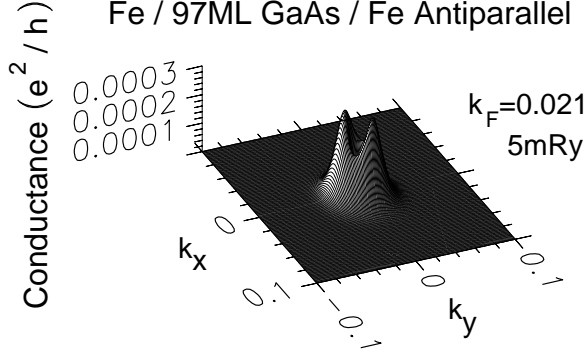


FIG. 9: Conductance ( $\mathbf{k}_{\parallel}$ -resolved) of incoming majority electrons, in the case of a Fe/ 97ML GaAs /Fe junction with antiparallel magnetic orientation of the two Fe leads, for  $E = E_c + 5\text{mRy}$ ,  $k_F = 0.021$ ; a quadruplicate symmetry is evident. The  $\mathbf{k}_{\parallel}$  axes are along the  $\bar{\Gamma} - \bar{M}$  directions.

tering effects). This is true for  $\mathbf{k}_{\parallel}$  in certain directions of the surface Brillouin zone, *i.e.* along  $k_x$  and  $k_y$  (the cubic axes), including of course  $\mathbf{k}_{\parallel} = 0$ . At such  $k$ -points, the transmission through the first interface (Fe into SC) is the same as through the second (SC into Fe); however, for other  $\mathbf{k}_{\parallel}$ -points this is not true, so spin-up and spin-down electrons have different  $g(\mathbf{k}_{\parallel})$  and only equal  $\mathbf{k}_{\parallel}$ -integrated  $g$  as shall be explained in the end of the section. Our numerical results verify this. So, for an arbitrary  $\mathbf{k}_{\parallel}$ -point, the geometric average relation can hold at most for the order of magnitude. We note in passing that, if we had a spacer material with  $C_{4v}$  interface symmetry, as *e.g.* MgO, the geometric average rule would not hold at all, because the minority Fe  $\Delta_{2'}(C_{4v})$ -state would be orthogonal to the spacer  $\Delta_1(C_{4v})$  conduction band; then the minority electrons would reach the second interface only through a complex band with exponentially damped probability and the assumptions of the two-reflectance-argument would not hold.

For a large spacer thickness of 97MLs we see in Fig. 9 the  $\mathbf{k}_{\parallel}$ -resolved conductance for the transmission from incoming majority-spin to outgoing minority-spin channels. In Table I, we see the integrated (over the SBZ) conductance for several gate voltage parameters  $E_0$  in the case of 97ML-thick spacers, together with the spin current polarisation  $P = (g_{\uparrow\uparrow} - g_{\downarrow\downarrow})/(g_{\uparrow\uparrow} + g_{\downarrow\downarrow})$  and the magnetoresistance (MR) ratio defined as  $(g_{\downarrow\uparrow} + g_{\uparrow\downarrow})/(g_{\uparrow\uparrow} + g_{\downarrow\downarrow})$  (the so-called “pessimistic definition”). Evidently the calculated device acts as an almost ideal spin filter and switch with extremely high MR ratio. For lower energy shifts the spin filtering and MR ratio increase, because the allowed  $\mathbf{k}_{\parallel}$  close up to  $\bar{\Gamma}$  and the states have more and more  $\Delta_1(C_{2v})$ -character. Because of the  $\Delta_{2'}$  minority-spin state, however, the ideal 100% cannot be reached even in the limiting case; in contrast, it would be reached *e.g.* in the case of an MgO spacer because it exhibits  $C_{4v}$ -symmetry.<sup>49</sup>

As promised at the end of the previous section, we

now turn our attention to the explanation of the circularly symmetric form of  $g(\mathbf{k}_{\parallel})$  for the majority electrons in the parallel-alignment case, vs. the octuple symmetry seen for the minority electrons, and all this vs. the quadruplicate symmetry in the antiparallel-alignment case. As  $\mathbf{k}_{\parallel}$  departs from  $\bar{\Gamma}$ , the Fe and SC states do not belong exclusively to a single representation any more, but are rather admixtures of the various representations; but they still retain mostly the character they had at  $\bar{\Gamma}$ . In the language of localised orbitals, the majority-spin states are formed mostly by the circularly symmetric  $s + p_z + d_{z^2}$  orbitals (plus small admixtures away from  $\bar{\Gamma}$ ); the minority-spin states consist of  $d_{xy}$  from the  $\Delta_{2'}(C_{4v})$ -band,  $p_x + p_y + d_{xz} + d_{yz}$  from the  $\Delta_5(C_{4v})$ -band, and  $d_{x^2-y^2}$  from the  $\Delta_2(C_{4v})$ -band; finally the SC conduction band states consist of  $s + p_z + d_{xy}$  from the  $\Delta_1(C_{2v})$ -band. Away from  $\bar{\Gamma}$ , new orbitals start to contribute to each band, but in amounts negligible for our discussion, since we remain close to  $\bar{\Gamma}$ .

Firstly we concentrate on the coupling of the minority-spin states. At exactly  $\bar{\Gamma}$ , the only combination that gives nonzero inner product is  $d_{xy}$  orbitals of Fe with  $d_{xy}$ -like states of the SC; the rest of the combinations are inner products of symmetric with antisymmetric wavefunctions, resulting to zero. As  $\mathbf{k}_{\parallel}$  departs from  $\bar{\Gamma}$ , the  $p_x, p_y, d_{xz}, d_{yz}$ , and  $d_{x^2-y^2}$  minority states of Fe atoms neighbouring a particular SC atom at the interface obtain slightly position-dependent phases as  $e^{i\mathbf{k}_{\parallel}\mathbf{r}}$ ; then the wavefunctions formed by combining them obtain a small part symmetric around the SC atom, and this gives nonzero inner product with the SC  $s + p_z + d_{xy}$ . This overlap integral, in first approximation proportional to  $k_{\parallel}$ , is different for the various directions of  $\mathbf{k}_{\parallel}$ , following the pattern of  $d_{xy}$ . Clearly then the bonding and the conductance must have a quadruplicate symmetry in  $\mathbf{k}_{\parallel}$ -space, as does  $d_{xy}$  in real space. By inspection of the Fig. 7 we see an octuple symmetry. The explanation for the extra symmetry lies in the zincblende geometry and the directionality of the bonding. Indeed, as we enter the SC (*e.g.* ZnSe) from the one lead, we encounter Zn and then Se on the tetrahedral positions along the  $(x, y)$  diagonal; but as we leave it, we encounter Se and then Zn on the tetrahedral positions along the  $(x, -y)$ -diagonal. Thus, the directionality of the SC  $d_{xy}$ -like states and consequently the bonding and transmission properties of the two interfaces are equivalent but rotated by  $90^\circ$  to each other, so the combined transmission obeys one extra symmetry operation and is octuple.

Secondly we focus on the coupling of the majority-spin states. There the situation is simpler: Fe has only  $s + p_z + d_{z^2}$  circularly symmetric orbitals which can couple only to the SC  $s + p_z$ , but not to  $d_{xy}$ . Thus no directionality is induced by the latter; even as we depart from  $\bar{\Gamma}$ , the small difference in phase obtained by neighbouring Fe sites gives only an antisymmetric part to the combined wavefunction and this has still zero inner product with the SC  $s + p_z + d_{xy}$ . The result is that the bonding and transmission properties for majority are isotropic

TABLE I: Calculated current polarisation and magnetoresistance (MR) ratio in the case of 97ML-thick spacers of ZnSe and GaAs for several gate voltage shifts  $E_F - E_c$ ; both are close to the ideal 100%. The spin-dependent conductance  $g$  integrated over the surface Brillouin zone is also shown for both cases of magnetic orientation of the leads: parallel (majority and minority) and antiparallel per spin (the same for the two spin channels).

Material	$E_F - E_c$	$g(e^2/h)$ (per unit-cell surface area)			Polarization	MR ratio
		Majority	Minority	Antiparallel/spin		
GaAs	5mRy (68meV)	$1.6 \times 10^{-7}$	$1.0 \times 10^{-12}$	$2.6 \times 10^{-10}$	99.999%	99.678%
	10mRy (136meV)	$7.1 \times 10^{-7}$	$2.1 \times 10^{-11}$	$2.7 \times 10^{-9}$	99.994%	99.229%
	20mRy (272meV)	$1.9 \times 10^{-6}$	$5.3 \times 10^{-11}$	$7.8 \times 10^{-9}$	99.994%	99.196%
ZnSe	5mRy (68meV)	$1.7 \times 10^{-7}$	$2.4 \times 10^{-12}$	$2.0 \times 10^{-9}$	99.972%	97.746%
	10mRy (136meV)	$8.2 \times 10^{-7}$	$3.0 \times 10^{-10}$	$1.4 \times 10^{-8}$	99.926%	96.553%
	20mRy (272meV)	$2.8 \times 10^{-6}$	$2.4 \times 10^{-9}$	$6.7 \times 10^{-8}$	99.823%	95.128%

around  $\bar{\Gamma}$ .

Finally we look at the antiparallel magnetic configuration of the leads. There, one either enters with circularly symmetric transmission via majority and exits with the quadruplicate symmetry via minority with a quadruplicate net result, as seen in Fig. 9, or, for the opposite spin, enters with quadruplicate symmetry via minority and exits with circularly symmetric transmission via majority, again with a quadruplicate net result. For the two last cases, by the way, the  $g(\mathbf{k}_{\parallel})$  are rotated to each other by  $90^\circ$ , again due to the aforementioned direction difference in the bonding; thus only along  $k_x$  and  $k_y$  is  $g(\mathbf{k}_{\parallel})$  the same for the two spin directions in the antiparallel case.

The same symmetry of  $g(\mathbf{k}_{\parallel})$  as here is seen in results for tunneling Fe/ZnSe/Fe junctions,<sup>25</sup> so once more we see the formal connection between spin injection and tunneling.

## VIII. LIMITATIONS AND SUMMARY

Before summarising, we shall briefly discuss the limitations of our approach and the relevance to realistic experimental situations. Two main points must be addressed here: (i) the influence of diffuse,  $\mathbf{k}_{\parallel}$ -violating scattering and (ii) the possible effect of a Schottky barrier. As for point (i), it is true that the formation of terraces or steps and interdiffusion lead to diffuse scattering. To what extent this reduces the control over the conductance must be examined separately in each case and is a huge but challenging task. In the case of the Fe/GaAs interface it is known that in growing of Fe on GaAs the As atoms act like surfactants forming always an As monolayer on Fe. This is of course an indication that the interface structure is not perfect. But progress is being done and one can reasonably hope that the quality of the interfaces will increase a lot in the future.

About point (ii), Schottky barriers are known to extend over mesoscopic lengths, especially when the doping is low. However, techniques to use quantum well structures have resulted in lowering the conduction band un-

der the Fermi level without direct impurity doping; such a situation would be modeled by our “gate voltage” parameter  $E_0$  in addition to a real gate voltage. Then the Schottky barrier would be much shorter, in fact being determined by the Fermi level pinning due to the metal-induced gap states. On the other hand, in the single-interface calculations for spin injection by Wunnicke *et al.*<sup>24</sup> the effect of a Schottky barrier has been studied by emulating it with a long region near the interface where the SC potentials were kept to their physical unshifted positions, and the electrons had to really tunnel into the conduction band. The result was quite encouraging, giving still an extremely high current spin polarisation.

To summarise, we have performed *ab initio* calculations of the spin-dependent transport through Fe/GaAs/Fe and Fe/ZnSe/Fe (001) junctions, with a gate voltage parameter acting on the semiconductor so that the Fermi level lies slightly in the conduction band. The electron transport was supposed to be completely ballistic, assuming a perfect interface structure and two-dimensional periodicity perpendicular to the direction of growth. Under these assumptions we have shown that such systems can exhibit an extremely high degree of current spin polarisation and also a magnetoresistance ratio approaching the ideal 100%. We have been able to trace down these nice properties to the difference in the bulk band structure for the two spin directions of Fe, and also to the difference in the bonding of majority- and minority-spin states at the interface with the semiconductor. In the same terms we have explained the high magnetoresistance values. We have also examined interesting interference effects that show up in such a junction due to the presence of two, rather than one, interfaces, and discussed the question whether these effects can invert the detected current polarisation.

We have seen that the understanding of these systems stands in close connection with the understanding of ballistic magnetic tunnel junctions, if one formally replaces the band structure near the center of the conduction band of the semiconductor with the complex band structure in the gap region. In both cases, it is important that very few states perform the conduction, namely the ones

near the center of the surface Brillouin zone; to know the properties of these states means to have control over the conductance.

We have concluded that the control over the desired properties of such systems is best when one deals with ballistic transport. Diffuse scattering, particularly at the interface, would intermix the various conducting channels and cause the injection efficiency and magnetoresistance to drop; on the other hand, clean and abrupt interfaces preserve  $\mathbf{k}_{\parallel}$  and act as spin-selective transmitters and

detectors.

### Acknowledgments

The authors gratefully acknowledge support from the RT Network of *Computational Magnetoelectronics* (Contract No: RTN1-1999-00145) of the European Commission.

- 
- <sup>1</sup> G. A. Prinz, *Science* **282**, 1660 (1998).
  - <sup>2</sup> S. A. Wolf, D. D. Awschalom, R. A. Buhrman, J. M. Daughton, S. von Molnár, M. L. Roukes, A. Y. Chtchelkanova, D. M. Treger, *Science* **294**, 1488 (2001).
  - <sup>3</sup> S. Datta and B. Das, *Appl. Phys. Lett.* **56**, 665 (1990).
  - <sup>4</sup> J. M. Kikkawa and D. D. Awschalom, *Nature* **397**, 139 (1999).
  - <sup>5</sup> I. Malajovich, J. J. Berry, N. Samarth, and D. D. Awschalom, *Nature* **411**, 770 (2001).
  - <sup>6</sup> R. Fiederling, M. Keim, G. Reuscher, W. Ossau, G. Schmidt, A. Waag, and L. W. Molenkamp, *Nature* **402**, 787 (1999).
  - <sup>7</sup> Y. Ohno, D. K. Young, B. Beschoten, F. Matsukura, H. Ohno, and D. D. Awschalom, *Nature* **402**, 790 (1999).
  - <sup>8</sup> G. Schmidt, G. Richter, P. Grabs, C. Gould, D. Ferrand, and L. W. Molenkamp, *Phys. Rev. Lett.* **87**, 227203 (2001).
  - <sup>9</sup> P. R. Hammar, B. R. Bennett, M. J. Yang, and M. Johnson, *Phys. Rev. Lett.* **83**, 203 (1999).
  - <sup>10</sup> F. G. Monzon and M. Roukes, *J. Magn. Magn. Mater.* **198-199**, 632 (1999).
  - <sup>11</sup> S. Gardelis, C. G. Smith, C. H. W. Barnes, E. H. Linfield, and D. A. Ritchie, *Phys. Rev. B* **60**, 7764 (1999).
  - <sup>12</sup> A. T. Filip, B. H. Hoving, F. J. Jedema, B. J. van Wees, B. Dutta, and S. Borghs, *Phys. Rev. B* **62**, 9996 (2000).
  - <sup>13</sup> V. P. LaBella, D. W. Bullock, Z. Ding, C. Emery, A. Venkatesan, W. F. Oliver, G. J. Salamo, P. M. Thibado, M. Mortazavi, *Science* **292**, 1518 (2001).
  - <sup>14</sup> H. J. Zhu, M. Ramsteiner, H. Kostial, M. Wassermeier, H.-P. Schönher, and K. H. Ploog, *Phys. Rev. Lett.* **87**, 016601 (2001).
  - <sup>15</sup> H. X. Tang, F. G. Monzon, R. Lifshitz, M. C. Cross, and M. L. Roukes, *Phys. Rev. B* **61**, 4437 (2000).
  - <sup>16</sup> D. L. Smith and R. N. Silver, *Phys. Rev. B* **64**, 045323 (2001); O. E. Raichev and P. Debray, *Phys. Rev. B* **65**, 085319 (2002); R. Vlutters, O. M. J. van 't Erve, R. Jansen, S. D. Kim, J. C. Lodder, A. Vedyayev, and B. Dieny, *Phys. Rev. B* **65**, 024416, (2001).
  - <sup>17</sup> G. Schmidt, D. Ferrand, L. W. Molenkamp, A. T. Filip, and B. J. van Wees, *Phys. Rev. B* **62**, R4790 (2000).
  - <sup>18</sup> E. I. Rashba, *Phys. Rev. B* **62**, R16267 (2000).
  - <sup>19</sup> A. Fert and H. Jaffrès, *Phys. Rev. B* **64**, 184420 (2001).
  - <sup>20</sup> D. Grundler, *Phys. Rev. B* **63**, 161307(R) (2001).
  - <sup>21</sup> C.-M. Hu and T. Matsuyama, *Phys. Rev. Lett.* **87**, 66803 (2001).
  - <sup>22</sup> H. B. Heersche, Th. Schäpers, J. Nitta, and H. Takayanagi, *Phys. Rev. B* **64**, 161307(R), (2001).
  - <sup>23</sup> G. Kirczenow, *Phys. Rev. B* **63**, 54422 (2001).
  - <sup>24</sup> O. Wunnicke, Ph. Mavropoulos, R. Zeller, P. H. Dederichs, and D. Grundler, arXiv:cond-mat/0201280
  - <sup>25</sup> J. M. MacLaren, X.-G. Zhang, W. H. Butler, and X. Wang, *Phys. Rev. B* **59**, 5470 (1999).
  - <sup>26</sup> Ph. Mavropoulos, N. Papanikolaou, and P. H. Dederichs, *Phys. Rev. Lett.* **85**, 1088 (2000).
  - <sup>27</sup> R. Zeller, P. H. Dederichs, B. Újfalussy, L. Szunyogh, and P. Weinberger *Phys. Rev. B* **52**, 8807 (1995).
  - <sup>28</sup> N. Papanikolaou, R. Zeller, and P. H. Dederichs, *J. Phys. Condens. Mat.* **14**, 2799 (2002).
  - <sup>29</sup> K. Wildberger, R. Zeller, and P. H. Dederichs, *Phys. Rev. B* **55**, 10074 (1997).
  - <sup>30</sup> R. Landauer, *IBM J. Res. Dev.* **1**, 233 (1957); R. Landauer, *Philos. Mag.* **21**, 863 (1970).
  - <sup>31</sup> M. Büttiker, *Phys. Rev. Lett.* **57**, 1761 (1986); M. Büttiker, *IBM J. Res. Dev.* **32**, 317 (1988).
  - <sup>32</sup> H. U. Baranger and A. D. Stone, *Phys. Rev. B* **40**, 8169 (1989).
  - <sup>33</sup> Ph. Mavropoulos, N. Papanikolaou, and P. H. Dederichs, unpublished.
  - <sup>34</sup> R. H. Parmenter, *Phys. Rev.* **100**, 573 (1955).
  - <sup>35</sup> M. Julliere, *Phys. Lett.* **54A**, 225 (1975).
  - <sup>36</sup> See, e.g., L. I. Schiff, *Quantum Mechanics*, 3. Ed., McGraw-Hill 1968, pp. 101-105.
  - <sup>37</sup> F. Mireles and G. Kirczenow, *Phys. Rev. B* **64**, 024426 (2001).
  - <sup>38</sup> Th. Schäpers, J. Nitta, H. B. Heersche, and H. Takayanagi, *Phys. Rev. B* **64**, 125314 (2001).
  - <sup>39</sup> P. Bruno, *Phys. Rev. B* **52**, 411 (1995).
  - <sup>40</sup> T. Taniguchi and M. Büttiker, *Phys. Rev. B* **60**, 13814 (2001).
  - <sup>41</sup> W. H. Butler, X.-G. Zhang, T. C. Schulthess, and J. M. MacLaren, *Phys. Rev. B* **63**, 054416 (2001).
  - <sup>42</sup> J. Mathon and A. Umerski, *Phys. Rev. B* **63**, 220403(R) (2001).
  - <sup>43</sup> Similar interference resonances in  $g(\mathbf{k}_{\parallel})$  have been observed in calculations of tunneling junctions,<sup>41</sup> for transmission through those evanescent states that also have a nonzero real  $k_z$ . Of course there the transmission probability is always many orders of magnitude smaller than one.
  - <sup>44</sup> Recent theoretical articles<sup>37,38</sup> based on model calculations have suggested that a modulation of the current polarisation due to interference by variation of  $k_F$  is possible. Our arguments deny this possibility for the systems considered here, but surely not for *all* systems. Note that Refs. 37 and 38 refer to systems of lower dimensionality (2D or 1D), where the averaging over  $\mathbf{k}_{\parallel}$  has a lesser effect (or is nonexistent, in 1D). Also, the aforementioned modulation

would be perhaps possible also in 3D if the minority-spin reflectance of the interface were lower.

<sup>45</sup> The situation is analogous to the one-dimensional case of a free electron of wavenumber  $k_{\text{in}} = \sqrt{E}$  encountering an infinitely long step barrier of height  $V_0$  where the wavenumber is  $k_{\text{out}} = \sqrt{E - V_0}$ . The transmission probability there is  $T_{\text{si}} = 4k_{\text{out}}k_{\text{in}}/(k_{\text{out}} + k_{\text{in}})^2$  going to zero as  $\sqrt{E - V_0}$  for small  $k_{\text{out}}$ . The point is that the group velocity in the barrier region goes to zero, although the transmission amplitude  $t$  remains finite, so current conservation forces  $T_{\text{si}} = |t|^2 k_{\text{out}}/k_{\text{in}}$  also to go to zero. The same point is true in our case when we approach the conduction band edge,<sup>24</sup> and thus the analogy is valid.

<sup>46</sup> This applies also for the  $k_{\parallel}$ -dependence of  $g$ : one sees the multi-resonant form of Fig. 2 if one substitutes the value for  $T_{\text{si}}(k_{\parallel} = 0)$  taken from the single interface calculation into eq. (12), and takes for the other  $\mathbf{k}_{\parallel}$ 's  $T_{\text{si}}(\mathbf{k}_{\parallel}) = T_{\text{si}}(0)k_z/k_F = T_{\text{si}}(0)\sqrt{k_F^2 - k_{\parallel}^2}/k_F$ ; in such an approxima-

tion, of course, any anisotropy of  $T_{\text{si}}(\mathbf{k}_{\parallel})$  is lost.

<sup>47</sup> This small imaginary part  $\epsilon$ , in principle infinitesimal, can also be viewed as imposing an attenuation  $\exp(-\sqrt{\epsilon}D)$  on the waves crossing a spacer of thickness  $D$ . Its effect can be studied by replacing  $t_2 \rightarrow t_2 \exp(-\sqrt{\epsilon}D)$  and  $r_2 \rightarrow r_2 \exp(-2\sqrt{\epsilon}D)$  in eq. (10). It turns out that the resonance maxima are then reduced for larger thicknesses, and that the reduction is stronger for smaller  $T_{\text{si}}$ . Thus the minority-spin conduction maxima are much more affected.

<sup>48</sup> Actually, the maxima in the DOS do not always have to coincide with those in the transmission; a relative phase shift can occur, as pointed out in Ref. 40. However, such a shift is not expected in the present case if we follow the analysis of Ref. 40, since there are no zeros of the transmission.

<sup>49</sup> The situation bears again an analogy with the magnetic tunnel junctions; in the limit of large spacer thickness, the current polarisation and MR ratio do not reach 100% for ZnSe,<sup>25</sup> but they do reach it for MgO.<sup>41,42</sup>